

Magnetic dipole excitation and its sum rule in nuclei with two valence nucleons

Tomohiro Oishi^{1,*} and Nils Paar^{1,†}

¹*Department of Physics, Faculty of Science, University of Zagreb, Bijenička c. 32, 10000 Zagreb, Croatia*

Background: Magnetic dipole (M1) excitation is the leading mode of nuclear excitation by the magnetic field, which couples unnatural-parity states. Since the M1 excitation occurs mainly for open-shell nuclei, the nuclear pairing effect is expected to play a role. As expected from the form of operator, this mode may provide the information on the spin-related properties, including the spin component of dineutron and diproton correlations.

Purpose: To investigate the M1 excitations of the systems with two valence nucleons above the closed-shell core, with pairing correlation included, and to establish for the first time the M1 sum rule that could be used to validate theoretical and experimental approaches. Possibility to utilize the M1 excitation as the probe of the dinucleon correlation is also discussed.

Method: Three-body model, which consists of a rigid spherical core and two valence nucleons, is employed. Interactions for its two-body subsystems are phenomenologically determined in order to reproduce the two-body and three-body energies. We also derive the M1 sum rule within the three-body picture.

Conclusion: The three-body model shows a significant role of the pairing correlation to suppress the M1 transition strength. The introduced M1 sum rule represents an important benchmark for the model calculations, and it provides a suitable probe for the effects of pairing in the systems with two valence nucleons. Therefore, further experimental studies of M1 transitions in those systems are called for.

PACS numbers: 21.10.-k, 21.45.+v, 23.20.-g, 23.20.Lv

I. INTRODUCTION

Electromagnetic excitations in finite nuclei are fundamental in nuclear physics and astrophysics. They provide valuable probe of the nuclear structure and dynamics and play a decisive role in the processes in stellar environments. In particular, magnetic dipole (M1) transitions have invoked various interests and discussions in recent studies [1–4]. The M1 excitation mode is relevant to a diversity of nuclear properties, including unnatural-parity states, spin-orbit splitting, tensor force effect, etc. Several collective nuclear phenomena, including scissors mode in deformed nuclei, can be activated by the M1 transitions [5–14]. In addition, the correspondence between the M1 and the zeroth component of Gamow-Teller (GT) modes has been discussed [10, 15, 16]: the M1 excitation can be utilized to optimize theoretical methods to predict the GT resonance distribution, which plays an essential role in neutrino-nucleus scattering.

Within a shell-model picture, the M1 transition couples spin-orbit partner orbits. Thus, this process is measurable mainly in open-shell nuclei, where the transition from the lower to higher partner orbit is available [5–7, 17–23]. In such systems, nuclear pairing correlation can play an essential role [24–27]. However, compared with the electric dipole (E1) and quadrupole (E2) modes [28–34], the knowledge on the pairing effect on magnetic modes, as well as on unnatural-parity states, is rather limited [10–12, 20].

In this work, we focus on the M1 excitation with a strong pairing, by employing the three-body model. This model is applicable to nuclei composed of the closed-shell core and two valence nucleons. For the purpose of this study, the sum rule for M1 transition is also introduced in this model assumption. We note that so far the corresponding sum rule has not been established. Indeed, in contrast to the electric multipole modes and GT resonance, whose sum rules of the excitation strength have been well established [35–40], general version of the M1 sum rule is not trivial. As a tentative solution in this situation, even it is still case-limited, our M1 sum rule may provide one standard to benchmark the theoretical investigation to some nuclei, where the three-body picture can be a good approximation.

It is worthwhile to mention so-called dineutron and diproton correlations, which can be relevant to our interest. Several theoretical studies have predicted that, under the effect of the pairing correlation, the valence two-nucleon subsystem may have a spin-singlet ($S = 0$) and/or spatially localized structure [28, 41–47]. However, considering its measurability, there remain some problems to clarify this intrinsic structure [48–50]. As expected from the form of the M1 transition operator, it may provide a suitable way to probe the total spin of nucleons, which should reflect the pairing effect inside nuclei.

The theoretical formalism, as well as numerical methods, are described in Sec. II. Then, section III is devoted to present our results and discussion. Finally, the summary and conclusion of this work are given in Sec. IV. The CGS-Gauss system of units is used in this article.

* E-mail: toishi@phy.hr

† E-mail: npaar@phy.hr

II. THREE-BODY MODEL

We employ the three-body model, which has been developed in Refs. [28, 43–47, 51–54]. Namely, the system consists of a rigid-core nucleus and two valence nucleons with the following assumptions.

- Core nucleus is spherical, i.e., with the shell-closure and $J^\pi = 0^+$. Nucleons in the core are not active for excitation.
- Two valence nucleons are of the same kind, namely, protons or neutrons. They feel the mean field, V_C , by the core nucleus.

Thus, the three-body Hamiltonian reads

$$H = h_C(1) + h_C(2) + v_{NN}(\mathbf{r}_1, \mathbf{r}_2) + x_{\text{rec}}, \quad (1)$$

$$h_C(i) = \frac{p_i^2}{2\mu_i} + V_C(\mathbf{r}_i), \quad (2)$$

$$x_{\text{rec}} = \frac{\mathbf{p}_1 \cdot \mathbf{p}_2}{m_C} \quad (\text{recoil term}), \quad (3)$$

where $i = 1$ (2) indicates the first (second) valence nucleon. The single-particle (SP) Hamiltonian, h_C , contains the mass parameters, $\mu_i = m_N m_C / (m_N + m_C)$, $m_N = 939.565$ (938.272) MeV/c² for neutrons (protons), and m_C of the core nucleus. Note that the recoil term also exists after the center-of-mass motion is subtracted. The SP potential, V_C , and the pairing potential, v_{NN} , are determined in the next section.

The SP state, $\psi_{nljm}(\mathbf{r}) = R_{nlj}(r) \cdot \mathcal{Y}_{ljm}(\theta, \phi)$, is solved to satisfy

$$h_C(i) \psi_{n_il_ij_im_i}(\mathbf{r}_i) = e_i \psi_{n_il_ij_im_i}(\mathbf{r}_i). \quad (4)$$

We employ the SP states up to the $h_{11/2}$ channel. In order to take into account the Pauli principle, we exclude the states occupied by the core. Continuum states are discretized within a box, $R_{\text{box}} = 30$ fm. The cutoff energy, $E_{\text{cut}} = 30$ MeV, is also employed to truncate the model space. We checked that this truncation indeed provides a sufficient convergence for results in the following sections.

For diagonalization of the total Hamiltonian, we employ the anti-symmetrized two-particle (TP) states for basis. That is, $\tilde{\Psi}_{k_1 k_2}^{(J,M)}(\mathbf{r}_1, \mathbf{r}_2) \equiv \hat{\mathcal{A}} \Psi_{k_1 k_2}^{(J,M)}(\mathbf{r}_1, \mathbf{r}_2)$, where

$$\begin{aligned} & \Psi_{k_1 k_2}^{(J,M)}(\mathbf{r}_1, \mathbf{r}_2) \\ & \equiv \sum_{m_1 m_2} \mathcal{C}_{m_1 m_2}^{(J,M)j_1 j_2} \psi_{n_1 l_1 j_1 m_1}(\mathbf{r}_1) \psi_{n_2 l_2 j_2 m_2}(\mathbf{r}_2). \end{aligned} \quad (5)$$

Here we take the short-hand label, $k_i \equiv \{n_i l_i j_i\}$.

The M1 operator, which operates only on the two valence nucleons, reads

$$\hat{Q}_\nu = \hat{q}_\nu(1) + \hat{q}_\nu(2), \quad (6)$$

where

$$\begin{aligned} \hat{q}_{\nu=0} &= \mu_N \sqrt{\frac{3}{4\pi}} (g_l \hat{l}_0 + g_s \hat{s}_0), \\ \hat{q}_{\nu=\pm 1} &= (\mp) \mu_N \sqrt{\frac{3}{4\pi}} (g_l \hat{l}_\pm + g_s \hat{s}_\pm). \end{aligned} \quad (7)$$

Notice that $\hat{l}_0 = \hat{l}_z$, $\hat{l}_\pm = (\hat{l}_x \pm i\hat{l}_y)/\sqrt{2}$, and similarly for the spin operators. As well known, g factors are given as $g_l = 1$ (0), and $g_s = 5.586$ (-3.826) for the proton (neutron) [35, 36]. In the following, we omit the nuclear magneton μ_N and the factor $\sqrt{3/4\pi}$, except when it needs.

A. M1 sum rule

The sum-rule value (SRV) of M1 transitions is determined as

$$\begin{aligned} S_{\text{M1}} &\equiv \sum_f \left(\left| \langle f | \hat{Q}_0 | i \rangle \right|^2 \right. \\ &\quad \left. + \left| \langle f | \hat{Q}_+ | i \rangle \right|^2 + \left| \langle f | \hat{Q}_- | i \rangle \right|^2 \right), \end{aligned} \quad (8)$$

where $|i\rangle$ and $|f\rangle$ indicate the initial and final states, respectively. Within the three-body model, because only two nucleons are available to excite, this can be reduced to

$$\begin{aligned} S_{\text{M1}} &= \left\langle i \left| \left(g_l \hat{\mathbf{L}} + g_s \hat{\mathbf{S}} \right)^2 \right| i \right\rangle \\ &= (g_l^2 - g_l g_s) \left\langle \hat{\mathbf{L}}^2 \right\rangle^{(i)} + (g_s^2 - g_l g_s) \left\langle \hat{\mathbf{S}}^2 \right\rangle^{(i)} \\ &\quad + g_l g_s \left\langle \hat{\mathbf{J}}^2 \right\rangle^{(i)}, \end{aligned} \quad (9)$$

where $\hat{\mathbf{J}} = \hat{\mathbf{L}} + \hat{\mathbf{S}}$, $\hat{\mathbf{L}} = \hat{l}(1) + \hat{l}(2)$, and $\hat{\mathbf{S}} = \hat{s}(1) + \hat{s}(2)$. Namely, the SRV contains the information on the coupled spins of the valence nucleons at the initial state.

Considering the simplification of the M1 sum rule, there are two cases, which can be especially worth mentioning.

- For two neutrons with $g_l = 0$, SRV is simply determined from the initial spin-triplet component, $N_{S=1}^{(i)}$:

$$\begin{aligned} S_{\text{M1}}(2\text{n}) &= g_s^2 \left\langle \hat{\mathbf{S}}^2 \right\rangle^{(i)} \\ &= g_s^2 \sum_{S=0,1} S(S+1) N_S^{(i)} = 2g_s^2 N_{S=1}^{(i)}. \end{aligned} \quad (10)$$

Notice that this spin-triplet component itself stands independently of the final-state properties.

- When two protons or neutrons are coupled to $J_i = 0$ at the initial state $|i\rangle$, Eq. (9) can be remarkably

simplified. In this case, in terms of the LS -coupling scheme, the allowed components include $(L, S) = (1, 1)$ and $(0, 0)$, only. Thus,

$$S_{\text{M1}}(J_i = 0) = 2(g_l - g_s)^2 N_{(L=1, S=1)}^{(i)}, \quad (11)$$

where we have utilized that the first-component, $N_{(L=1, S=1)}^{(i)}$, can be identical to $N_{L=1}^{(i)}$ as well as $N_{S=1}^{(i)}$.

Notice that, in both cases, the M1 SRV is enhanced (suppressed) when the $S = 1$ ($S = 0$) component is dominant.

B. no-pairing SRV

It is worthwhile to mention the SRV in one special case, where the non-diagonal terms in the Hamiltonian can be neglected: $H \rightarrow H_{\text{NP}} = h_C(1) + h_C(2)$. In this case, the SRV can be analytically obtained. Because of the diagonal Hamiltonian, the initial state with the total angular momentum J_i should be solved as the single set of coupled SP states. That is,

$$|i\rangle = [|l_1 j_1\rangle \otimes |l_2 j_2\rangle]^{(J_i)}, \quad (12)$$

where l_k and j_k indicate the angle-quantum numbers of the k th valence nucleon. Thus, Eq. (9) is represented as

$$S_{\text{M1, NP}} = (g_l^2 - g_l g_s) \sum_{L=|l_1-l_2|}^{l_1+l_2} L(L+1) N_L^{(l_1 j_1, l_2 j_2; J_i)} + (g_s^2 - g_l g_s) 2N_{S=1}^{(l_1 j_1, l_2 j_2; J_i)} + g_l g_s J_i(J_i+1), \quad (13)$$

where $N_X^{(l_1 j_1, l_2 j_2; J_i)}$ indicates the contribution of the X component in this initial state. The analytic derivation of $N_X^{(l_1 j_1, l_2 j_2; J_i)}$ for an arbitrary set of $(l_1, j_1, l_2, j_2, J_i)$ can be found in, e.g. textbook [55]. This no-pairing, analytic SRV can provide a solid standard to benchmark one's theoretical model, as well as its computational implementation.

III. NUMERICAL RESULT

For numerical calculation, first we focus on the ^{18}O nucleus. Its core, ^{16}O , can be suitable to the rigid-core assumption.

A. no-pairing case

For simplicity, we first neglect the non-diagonal terms, v_{NN} and x_{rec} in Eq. (1), thus we deal with the no-pairing Hamiltonian, $H_{\text{NP}} = h_C(1) + h_C(2)$.

In the first step, we need to constrain the core-neutron potential, V_C , for the SP states by considering the core-neutron subsystem, ^{17}O . For this purpose, we employ the

Woods-Saxon (WS) potential:

$$V_C(\mathbf{r}) = V_0 f(r) + U_{ls}(\mathbf{l} \cdot \mathbf{s}) \frac{1}{r} \frac{df}{dr},$$

$$f(r) = \frac{1}{1 + e^{(r-R_0)/a_0}}, \quad (14)$$

where $R_0 = r_0 \cdot A_C^{1/3}$, $A_C = 16$, $r_0 = 1.25$ fm, $a_0 = 0.65$ fm, $V_0 = -53.2$ MeV, and $U_{ls} = 22.1$ MeV fm 2 . These parameters reproduce well the empirical SP energies of ^{17}O , as shown in Table I. Note that, due to the Pauli principle, we exclude from our basis $1s_{1/2}$, $1p_{3/2}$, and $1p_{1/2}$ states, which are occupied by the core.

In the following, we move to the core plus two-neutron system, ^{18}O . In the no-pairing case, the GS can be trivially solved as

$$\Psi_{\text{GS}}(\mathbf{r}_1, \mathbf{r}_2) = \hat{\mathcal{A}} [\psi_{1d_{5/2}}(\mathbf{r}_1) \otimes \psi_{1d_{5/2}}(\mathbf{r}_2)]^{(J_i=0)}, \quad (15)$$

which satisfies $H_{\text{NP}} |\Psi_{\text{GS}}\rangle = E_{\text{GS}} |\Psi_{\text{GS}}\rangle$ with $E_{\text{GS}} = 2e(1d_{5/2})$. Notice that, from Table I, this GS energy is $2e(1d_{5/2}) = -8.286$ MeV, which is higher than the empirical two-neutron binding energy, $B_{2n} = -12.188$ MeV, of ^{18}O [56]. This discrepancy is, of course, due to the no-pairing assumption.

We now compute the M1 excitation from the 0^+ ground state (GS). For 1^+ excited states, we solve all the TP states coupled to 1^+ : $H_{\text{NP}} |f(1^+)\rangle = E_f |f(1^+)\rangle$.

In Fig. 1, we plot the M1 transition strength:

$$B_{\text{M1}}(E_\gamma) = \sum_{\nu=0, \pm 1} \left| \langle f(1^+) | \hat{Q}_\nu | \Psi_{\text{GS}}(0^+) \rangle \right|^2, \quad (16)$$

where $E_\gamma = E_f - E_{\text{GS}}$. Note that, because the system is spherical, $\nu = 0$ and ± 1 yield the same result. The figure also shows the continuous distribution obtained by smearing the discrete strength with a Cauchy-Lorenz profile, whose full width at half maximum (FWHM) is 1.0 MeV.

In Fig. 1, the highest transition strength without pairing locates at $E_\gamma \cong 5$ MeV, which coincides well with the gap energy between the SP states $1d_{5/2}$ and $1d_{3/2}$. Thus, the transition $1d_{5/2} \rightarrow 1d_{3/2}$ plays a major role in this case.

The numerical SRV can be obtained from the sum of

TABLE I. Single-neutron energies for ^{17}O (in MeV). For the resonant $d_{3/2}$ level, its energy and width Γ are obtained by evaluating the scattering phase-shift.

	This work	Exp. [56]	Type
$e(1d_{5/2})$	-4.143	-4.143	bound
$e(2s_{1/2})$	-3.275	-3.272	bound
$e_r(d_{3/2})$	+0.902	+0.941	resonance
	$(\Gamma = 0.102)$	$(\Gamma = 0.096)$	

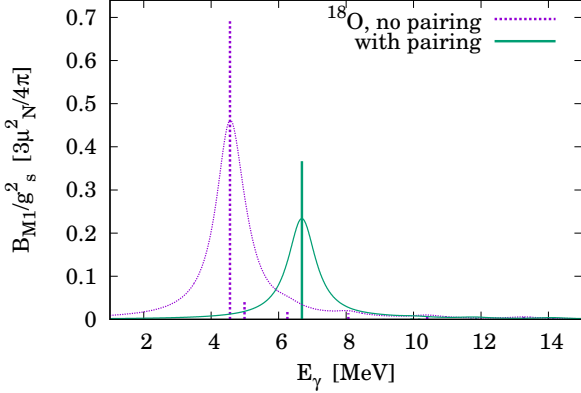


FIG. 1. Discrete M1 transition strength for ^{18}O . The continuous distribution is also plotted by smearing the discrete strength with a Cauchy-Lorenz profile, whose full width at half maximum (FWHM) is 1.0 MeV.

discrete M1 transition strength, resulting in,

$$S_{\text{M1,cal.}} = \sum_{E_\gamma} B_{\text{M1}}(E_\gamma) \cong 0.799 g_s^2. \quad (17)$$

On the other side, the corresponding analytic SRV for the $S = 1$ component reads from Eq. (13),

$$S_{\text{M1,NP}} = 2g_s^2 N_{S=1}^{(d_{5/2}, d_{5/2}; J=0)},$$

where the spin-triplet component $N_{S=1}^{(d_{5/2}, d_{5/2}; J=0)} = 2/5$, exactly [55]. Thus, our numerical SRV is consistent to the analytic one. Notice also that, in Fig. 1, the highest strength has $0.69g_s^2$, which exhausts about 87% of the total SRV. This again means a major component comes from $1d_{5/2} \rightarrow 1d_{3/2}$ transition.

B. pairing case

In the following, the non-diagonal terms of Hamiltonian, v_{NN} and x_{rec} , are also taken into account in the analysis of ^{18}O . For the pairing interaction, we employ a density-dependent contact (DDC) potential, similarly as in Refs. [28, 44, 46, 52, 53]. That is,

$$v_{NN}(\mathbf{r}_1, \mathbf{r}_2) = w(|\mathbf{R}_{12}|) \cdot \delta(\mathbf{r}_1 - \mathbf{r}_2), \\ w(r) = w_0 [1 - f(r)], \quad (18)$$

where $\mathbf{R}_{12} = (\mathbf{r}_1 + \mathbf{r}_2)/2$. The $f(r)$ is the same WS profile given in Eq. (14), and it schematically describes the density-dependence of the effective pairing interaction. Its bare strength is determined consistently from the neutron-neutron scattering length in vacuum, $a_v = -18.5$ fm, within the cutoff energy [52, 53]. That is,

$$w_0 = \frac{4\pi^2 \hbar^2 a_v}{m_n (\pi - 2a_v k_{\text{cut}})} \quad [\text{MeV} \cdot \text{fm}^3], \quad (19)$$

TABLE II. Ground-state properties for ^{18}O obtained with or without the DDC-pairing correlation plus recoil. Note that $E_{\text{GS}} = -12.188$ MeV in the experimental data [56].

	Pairing	No pair.
$E_{\text{GS}} = \langle H \rangle$	-12.019 MeV	-8.286 MeV
$\langle v_{NN} \rangle$	-4.337 MeV	0 MeV
$\langle x_{\text{rec}} \rangle$	-0.177 MeV	0 MeV
$N_{d_{5/2} \otimes d_{5/2}}$	89.9%	100%
$N_{S=1}$	19.7%	40%

where $k_{\text{cut}} = \sqrt{m_n E_{\text{cut}}}/\hbar$.

The two-neutron GS is solved by diagonalizing the three-body Hamiltonian via the anti-symmetrized TP basis coupled to 0^+ . As the result, the GS energy for ^{18}O is obtained, $E_{\text{GS}} = -12.019$ MeV, which is in fair agreement with the experimental value, -12.188 MeV [56]. The 1^+ excited states, on the other side, are solved by diagonalizing the same Hamiltonian, but via the 1^+ TP basis.

In Table II, properties of the 0^+ GS are summarized. One can read that the pairing correlation leads to the deeper binding of two neutrons. Furthermore, the GS cannot be pure $(d_{5/2})^2$ state, but it includes other components. As the result, the spin-triplet ($S = 1$) component is remarkably suppressed from the no-pairing case, similarly to the dineutron and diproton correlations [28, 46]. Note that this component is evaluated by numerically integrating the initial-state density, $|\Psi_{\text{GS}}(\mathbf{r}_1, \mathbf{r}_2)|^2$, but after the spin-triplet projection. That is,

$$N_{S=1} = \int d\mathbf{r}_1 \int d\mathbf{r}_2 \left| \hat{P}_{S=1} \Psi_{\text{GS}}(\mathbf{r}_1, \mathbf{r}_2) \right|^2, \quad (20)$$

whereas the density is normalized as $\sum_S N_S = 1$.

In Fig. 1, the M1 transition strength with pairing interaction is presented for ^{18}O . In comparison to the no-pairing case, a significant suppression of the transition strength is obtained. Also, we have checked that, beside the decrease of GS energy due to the pairing attraction, the excitation energies of M1 states are less sensitive on the pairing interaction. Thus, the main M1 peak is slightly shifted to the higher-energy region at $E_\gamma \cong 6.7$ MeV.

The numerical SRV is now obtained by integrating the strength distribution in Fig. 1. The result is,

$$S_{\text{M1,cal.}} = \sum_{E_\gamma} B_{\text{M1}}(E_\gamma) \cong 0.393 g_s^2, \quad (21)$$

with the pairing correlation. This value is, as expected from Eq. (10), consistent with the initial $S = 1$ component, $S_{\text{M1}}(2n) = 2g_s^2 N_{S=1}$, where $N_{S=1} = 0.197$ as evaluated by Eq. (20). Corresponding to the reduced M1 transition strength, the SRV is also suppressed by the pairing correlation. The typical reduction factor from the

no-pairing result is 0.5 in this ^{18}O case. Consequently, the M1 SRV as well as its strength is noticeably sensitive to the nuclear-pairing effect.

From the experimental side, there is no evidence of the 1^+ state in ^{18}O around 6.7 MeV, as predicted in Fig. 1. One possible reason is that our theoretical model does not quantitatively reproduce the 1^+ excited states. Especially, the 1^+ excitation energies may be sensitive to the pairing interaction model, which has, however, not been optimized specifically to this unnatural-parity transition case. One should mention that, from the experimental point of view, the M1 excitation of ^{18}O is rather weak and beyond the present level of measurability, because the number of valence neutrons is only two. This is in contrast to some nuclei [5–7, 17–23], where 10–20 valence nucleons can contribute to the M1 transition, and make its response sufficiently strong. For ^{18}O with the weak M1 excitation, the selective detection of 1^+ states is possibly demanding. One should consider, e.g. the dominance of the E1 mode, and the competition with the E2 mode. To extract the pure information on the M1 process from existing data, further efforts may be necessary. We leave these issues for the future study.

C. mirror nucleus ^{18}Ne

Next we investigate the M1 excitations of the mirror nucleus, ^{18}Ne , as the ^{16}O core plus two valence protons with the Coulomb repulsion. Some parameters in the three-body model are revised to take the mass m_p , different g factors, and Coulomb repulsion into account. For the Coulomb repulsion, the same procedure as in Refs. [34, 46] is utilized. That is, for the core-proton subsystem, we additionally employ the Coulomb potential of an uniformly-charged sphere. Also, for the proton-proton interaction, the reduction factor, $f = 0.96$, is used for $v_{pp} = f \cdot v_{NN}$, in order to reproduce the empirical two-proton separation energy. Other parameters are kept unchanged from the ^{18}O case.

Our results are summarized in Fig. 2 and Table III. Indeed, one can observe similar behavior of the M1 transition strength, i.e., it is suppressed when the pairing correlation exists. This conclusion coincides with the reduction of the spin-triplet component in the GS by the pairing, as shown in Table. III.

The numerical SRVs with and without the pairing correlation are obtained as $S_{\text{M1,cal.}} = 0.402(g_l - g_s)^2$ and $0.799(g_l - g_s)^2$, respectively. Thus, the typical reduction factor between the pairing and no-pairing SRVs is similar in the isobaric analogue systems, ^{18}O and ^{18}Ne . We also note that the no-pairing SRV is consistent to the analytic solution, $4(g_l - g_s)^2/5$.

TABLE III. Same as Table II, but for ^{18}Ne . Note that $E_{\text{GS}} = -4.523$ MeV in the experimental data [56].

	Pairing	No pair.
$E_{\text{GS}} = \langle H \rangle$	-4.527 MeV	-1.154 MeV
$\langle v_{pp} \rangle$	-3.928 MeV	0 MeV
$\langle x_{\text{rec}} \rangle$	-0.144 MeV	0 MeV
$N_{d_{5/2} \otimes d_{5/2}}$	89.3%	100%
$N_{S=1}$	20.2%	40%

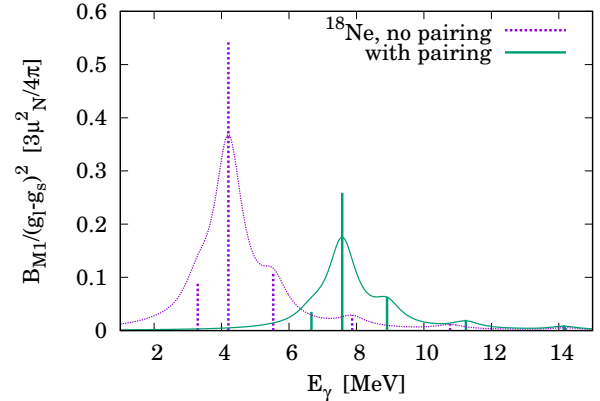


FIG. 2. Same as Fig. 1, but for ^{18}Ne .

D. pf -shell nucleus ^{42}Ca

In the last two cases, we investigated the M1 excitation of the nucleon pair from the sd shell. In the following, we move toward the pf -shell system, namely, ^{42}Ca , where the ^{40}Ca core corresponds to the shell-closure, and thus, it is suitable to our rigid-core assumption.

For the computation, we change some model parameters, $A_C = 40$, $V_0 = -55.7$ MeV, and $U_{ls} = 10.8$ MeV fm 2 . Other parameters in V_C , v_{NN} , and cutoff parameters remain the same as in the ^{18}O case. This setting fairly reproduces the single-neutron energies of $1f_{7/2}$ and $1f_{5/2}$ in ^{41}Ca [56]. Due to the Pauli principle, we exclude the SP states up to $1d_{3/2}$, which are occupied by the core.

The GS properties of ^{42}Ca are summarized in Table IV. Its GS energy is obtained as $E_{\text{GS}} = -19.232$ MeV, in a fair agreement with the empirical value, -19.843 MeV [56].

In Fig. 3, the M1 transition strength for ^{42}Ca is shown for the cases with and without pairing interaction. One can find qualitatively the same conclusion as in the sd -shell nuclei: the pairing correlation suppresses the strength of M1 transitions. The SRV with the pairing is obtained as $S_{\text{M1,cal.}} = 0.352g_s^2$. This result is, as expected from Eq. (10), consistent to the $S_{\text{M1}}(2\text{n}) = 2g_s^2 N_{S=1}$, where $N_{S=1} = 0.176$ as shown in

TABLE IV. Same as Table II, but for ^{42}Ca . Note that $E_{\text{GS}} = -19.843$ MeV in the experimental data [56].

	Pairing	No pair.
$E_{\text{GS}} = \langle H \rangle$	-19.232 MeV	-16.795 MeV
$\langle v_{NN} \rangle$	-2.999 MeV	0 MeV
$\langle x_{\text{rec}} \rangle$	-0.005 MeV	0 MeV
$N_{S=1}$	17.6%	42.9%

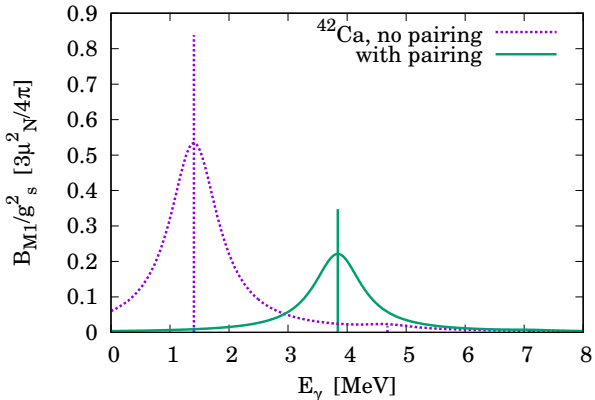


FIG. 3. Same as Fig. 1, but for ^{42}Ca .

Table IV. Similarly to the *sd*-shell case, the M1 SRV is shown to be linked with the coupled spin, which reflects the pairing effect.

IV. SUMMARY

We have investigated M1 excitations in the systems with two-valence nucleons in the framework of the three-

body model. First we have introduced model independent M1 sum rule, that is applicable to nuclei with two protons or neutrons above the core with the shell closure. We showed that the total sum of M1 transition strength can be linked directly to the spin-triplet component of the two valence nucleons in the shell. We also performed the three-body model calculations of M1 transition strength with the simple DDC-pairing interaction for ^{18}O , ^{18}Ne , and ^{42}Ca . Model calculations accurately reproduced the proposed M1 sum rule values. It is shown that the pairing correlation reduces the spin-triplet component of the initial state, and thus, the M1 excitation is correspondingly suppressed. The same conclusion applies both in the *sd* and *pf*-shell nuclei. Consequently, one can expect that the M1 excitation is a promising probe to investigate the spin structure of valence nucleons, including dineutron and diproton correlations.

From the experimental side, additional studies are necessary to extract the spin information from the M1 excitation data, in particular for the systems with two-valence nucleons above the closed-shell core, where the introduced M1 sum rule could be validated. The main problem is the contribution from other, electric modes, which lead to the hindrance against the M1 strength. A close collaboration between theory and experiment may be necessary to resolve this issue.

ACKNOWLEDGMENTS

T. Oishi sincerely thank T. O. Yamamoto for suggestions from the experimental side. This work is supported by the Croatian Science Foundation under the project Structure and Dynamics of Exotic Femtosystems (IP-2014-09-9159) and by the QuantiXLie Centre of Excellence, a project co financed by the Croatian Government and European Union through the European Regional Development Fund, the Competitiveness and Cohesion Operational Programme (KK.01.1.1.01).

[1] A. Richter, *Progress in Particle and Nuclear Physics* **13**, 1 (1985).
[2] U. Kneissl, H. Pitz, and A. Zilges, *Progress in Particle and Nuclear Physics* **37**, 349 (1996).
[3] N. Pietralla, P. von Brentano, and A. Lisetskiy, *Progress in Particle and Nuclear Physics* **60**, 225 (2008).
[4] K. Heyde, P. von Neumann-Cosel, and A. Richter, *Rev. Mod. Phys.* **82**, 2365 (2010), and references therein.
[5] D. Bohle, A. Richter, W. Steffen, A. Dieperink, N. L. Iudice, F. Palumbo, and O. Scholten, *Physics Letters B* **137**, 27 (1984).
[6] D. Bohle, G. Kchler, A. Richter, and W. Steffen, *Physics Letters B* **148**, 260 (1984).
[7] A. Richter, *Nuclear Physics A* **507**, 99 (1990).
[8] T. Otsuka, *Nuclear Physics A* **507**, 129 (1990).
[9] S. Kamerdzhiev and J. Speth, *Nuclear Physics A* **599**, 373 (1996), proceedings of the Groningen Conference on Giant Resonances.
[10] P. Vesely, J. Kvasil, V. O. Nesterenko, W. Kleinig, P. G. Reinhard, and V. Y. Ponomarev, *Phys. Rev. C* **80**, 031302 (2009).
[11] V. O. Nesterenko, J. Kvasil, P. Vesely, W. Kleinig, P.-G. Reinhard, and V. Y. Ponomarev, *Journal of Physics G: Nuclear and Particle Physics* **37**, 064034 (2010).
[12] V. O. Nesterenko, J. Kvasil, P. Vesely, W. Kleinig, and P.-G. Reinhard, *Int. J. Mod. Phys. E* **19**, 558 (2010).
[13] R. Schwengner, S. Frauendorf, and B. A. Brown, *Phys. Rev. Lett.* **118**, 092502 (2017).
[14] E. B. Balbutsev, I. V. Molodtsova, and P. Schuck, *Phys. Rev. C* **97**, 044316 (2018).
[15] K. Langanke, G. Martínez-Pinedo, P. von Neumann-Cosel, and A. Richter, *Phys. Rev. Lett.* **93**, 202501 (2004).
[16] J. Stone and P.-G. Reinhard, *Progress in Particle and*

Nuclear Physics **58**, 587 (2007).

[17] R. Moreh, S. Shlomo, and A. Wolf, Phys. Rev. C **2**, 1144 (1970).

[18] R. M. Laszewski, P. Rullhusen, S. D. Hoblit, and S. F. LeBrun, Phys. Rev. Lett. **54**, 530 (1985).

[19] R. M. Laszewski, R. Alarcon, D. S. Dale, and S. D. Hoblit, Phys. Rev. Lett. **61**, 1710 (1988).

[20] S. Kamerdzhev, J. Speth, G. Tertychny, and J. Wambach, Zeitschrift für Physik A **346**, 253 (1993).

[21] R. Fearick, G. Hartung, K. Langanke, G. Martnez-Pinedo, P. von Neumann-Cosel, and A. Richter, Nuclear Physics A **727**, 41 (2003).

[22] H. Pai, T. Beck, J. Beller, R. Beyer, M. Bhike, V. Derya, U. Gayer, J. Isaak, Krishichayan, J. Kvasil, B. Löher, V. O. Nesterenko, N. Pietralla, G. Martínez-Pinedo, L. Mertes, V. Y. Ponomarev, P.-G. Reinhard, A. Repko, P. C. Ries, C. Romig, D. Savran, R. Schwengner, W. Tornow, V. Werner, J. Wilhelmy, A. Zilges, and M. Zweidinger, Phys. Rev. C **93**, 014318 (2016).

[23] T. Shizuma, T. Hayakawa, I. Daito, H. Ohgaki, S. Miyamoto, and F. Minato, Phys. Rev. C **96**, 044316 (2017).

[24] D. Brink and R. Broglia, *Nuclear Superfluidity: Pairing in Finite Systems*, Cambridge Monographs on Particle Physics, Nuclear Physics and Cosmology (Cambridge University Press, Cambridge, UK, 2005).

[25] R. A. Broglia and V. Zelevinsky, eds., *Fifty Years of Nuclear BCS: Pairing in Finite Systems* (World Scientific, Singapore, 2013).

[26] D. J. Dean and M. Hjorth-Jensen, Rev. Mod. Phys. **75**, 607 (2003).

[27] M. Bender, P.-H. Heenen, and P.-G. Reinhard, Rev. Mod. Phys. **75**, 121 (2003).

[28] K. Hagino and H. Sagawa, Phys. Rev. C **72**, 044321 (2005).

[29] K. Yoshida, Phys. Rev. C **80**, 044324 (2009).

[30] J. Terasaki and J. Engel, Phys. Rev. C **84**, 014332 (2011).

[31] I. Stetcu, A. Bulgac, P. Magierski, and K. J. Roche, Phys. Rev. C **84**, 051309 (2011).

[32] S. Ebata, T. Nakatsukasa, and T. Inakura, Phys. Rev. C **90**, 024303 (2014).

[33] N. D. Dang and N. Q. Hung, Journal of Physics G: Nuclear and Particle Physics **40**, 105103 (2013).

[34] T. Oishi, K. Hagino, and H. Sagawa, Phys. Rev. C **84**, 057301 (2011).

[35] J. Eisenber and W. Greiner, *Nuclear Theory Volume 2: Excitation Mechanisms of the Nucleus* (North-Holland Publishing Company, Amsterdam, 1970).

[36] P. Ring and P. Schuck, *The Nuclear Many-Body Problems* (Springer-Verlag, Berlin and Heidelberg, Germany, 1980).

[37] S. Wang, Phys. Rev. A **60**, 262 (1999).

[38] Y. Lu and C. W. Johnson, Phys. Rev. C **97**, 034330 (2018).

[39] K. Ikeda, S. Fujii, and J. I. Fujita, Phys. Lett. **3**, 271 (1963).

[40] J. I. Fujita, S. Fujii, and K. Ikeda, Phys. Rev. **133**, 549 (1964).

[41] M. Matsuo, K. Mizuyama, and Y. Serizawa, Phys. Rev. C **71**, 064326 (2005).

[42] M. Matsuo, H. Shimoyama, and Y. Ootaki, Physica Scripta **T150**, 014024 (2012).

[43] C. A. Bertulani and M. S. Hussein, Phys. Rev. C **76**, 051602 (2007).

[44] K. Hagino, H. Sagawa, J. Carbonell, and P. Schuck, Phys. Rev. Lett. **99**, 022506 (2007).

[45] K. Hagino and H. Sagawa, Phys. Rev. C **89**, 014331 (2014).

[46] T. Oishi, K. Hagino, and H. Sagawa, Phys. Rev. C **82**, 024315 (2010), with erratum.

[47] T. Oishi, K. Hagino, and H. Sagawa, Phys. Rev. C **90**, 034303 (2014).

[48] K. Hagino and H. Sagawa, Few-Body Systems **57**, 185 (2016).

[49] Y. Kikuchi, K. Ogata, Y. Kubota, M. Sasano, and T. Uesaka, Progress of Theoretical and Experimental Physics **2016**, 103D03 (2016).

[50] L. V. Grigorenko, J. S. Vaagen, and M. V. Zhukov, Phys. Rev. C **97**, 034605 (2018), and references therein.

[51] Y. Suzuki and K. Ikeda, Phys. Rev. C **38**, 410 (1988).

[52] G. Bertsch and H. Esbensen, Annals of Physics **209**, 327 (1991).

[53] H. Esbensen, G. F. Bertsch, and K. Hencken, Phys. Rev. C **56**, 3054 (1997).

[54] L. Fortunato, R. Chatterjee, J. Singh, and A. Vitturi, Phys. Rev. C **90**, 064301 (2014).

[55] A. R. Edmonds, *Angular Momentum in Quantum Mechanics*, Princeton Landmarks in Physics (Princeton University Press, Princeton, USA, 1960).

[56] “Chart of Nuclides”, National Nuclear Data Center (NNDC); <http://www.nndc.bnl.gov/chart/>.